

Isotope Quantum Effects in the Metallization Transition in Liquid Hydrogen

Sebastiaan van de Bund¹, Heather Wiebe¹, and Graeme J. Ackland¹

School of Physics & Astronomy, The University of Edinburgh, Edinburgh EH9 3FD, United Kingdom



(Received 13 September 2020; revised 12 November 2020; accepted 21 April 2021; published 2 June 2021)

Quantum effects in condensed matter normally only occur at low temperatures. Here we show a large quantum effect in high-pressure liquid hydrogen at thousands of Kelvins. We show that the metallization transition in hydrogen is subject to a very large isotope effect, occurring hundreds of degrees lower than the equivalent transition in deuterium. We examined this using path integral molecular dynamics simulations which identify a liquid-liquid transition involving atomization, metallization, and changes in viscosity, specific heat, and compressibility. The difference between H₂ and D₂ is a quantum mechanical effect that can be associated with the larger zero-point energy in H₂ weakening the covalent bond. Our results mean that experimental results on deuterium must be corrected before they are relevant to understanding hydrogen at planetary conditions.

DOI: [10.1103/PhysRevLett.126.225701](https://doi.org/10.1103/PhysRevLett.126.225701)

Hydrogen, despite being the simplest element on the periodic table, exhibits rich physics at high pressures. Of particular interest is the insulator-to-metal transition, wherein the system transforms from an insulating molecular phase to a conducting phase. Extremely high static compression is required to reach the metallic solid [1,2], but transition to a metallic liquid has been observed in both static [3–6] and dynamic [7–9] compression experiments. This liquid-liquid phase transition (LLPT) is of vital importance to the modeling of the interior of Jovian-like planets [10–12], as the metallization of hydrogen is thought to cause the demixing of hydrogen and helium at pressure [13]. Despite this importance, the nature of the LLPT is not fully understood. The prevailing hypothesis is that the LLPT is a first order transition between an insulating molecular liquid and a conducting atomic one, terminating at a critical point between 1000 and 1500 K. This is supported by density functional theory (DFT) [14–18] and quantum Monte Carlo [19–22] simulations. However, a quantitative agreement between theory and experiment has not yet been achieved, and the consensus in modelling was recently challenged [23].

The hydrogen phase diagram exhibits features which are impossible in classical physics. Such features are typically only seen at low temperatures and involve nuclear quantum effects (NQE). One example is the solid “phase I” of hydrogen, which extends to zero temperature but involves freely rotating molecules. Then there is a significant difference between H₂ and D₂ in the low temperature phase boundary between phase I and the broken-symmetry phase II, in which both isotope mass and quantum spin statistics play a role [24].

However, “low-temperature” begs the question “low compared to what?” No isotope effect is known for the melting line in hydrogen, and nuclear quantum effects are

often ignored at the kiloKelvin temperatures of liquid hydrogen. The melting transition involves changes in intermolecular bonding, which is a relatively weak interaction. The LLPT, on the other hand, involves breaking the covalent bonds. The zero-point energy of H₂ is 78.46 meV (~910 K) higher than that of D₂ [25], and so the covalent bonding in H₂ is significantly weaker. Consequently, isotope effects at an unprecedentedly high temperature could be manifested in the experimentally observable difference in the LLPT phase boundary. Indeed, a 700 K difference in the LLPT phase lines of H₂ and D₂ was reported by Zaghoo *et al.* by monitoring reflectivity in a laser-heated diamond anvil cell [5]. Interestingly, a spectroscopic study conducted by Jiang *et al.* one year later did not detect an appreciable isotope effect [6].

There are numerous pitfalls in calculating the hydrogen LLPT (see Supplemental Material for further discussion [26]). Cheng *et al.* recently demonstrated how many previous studies with less than 250 atoms and trajectories several ps in length were stuck in a solid rather than molecular-liquid phase. Γ -only k -point sampling leads to unphysical chainlike “polyhydrogen” structures [56] and inclusion of NQE [19,21,22,27] is essential to finding any isotope effect because in classical theory, the phase boundaries of hydrogen and deuterium are identical [28]. Such a difference undermines the relevance of experiments on deuterium to determine the hydrogen equation of state—a crucial component of planetary and exoplanetary science.

Another challenge for DFT is that most exchange-correlation functionals cannot describe both molecular and metallic phases well, further contributing to the wide spread of results for the LLPT line from DFT (see Table S1 in Supplemental Material [26]). Functionals which do not correctly describe the high density limit of the exchange energy are particularly poor for describing molecule-atom

transitions [29]. Here we adopt the BLYP functional for the majority of our results [30,31] which has been shown to be the closest to Quantum Monte Carlo for molecular systems, including molecular metals which are problematic with PBE [32]. Nevertheless, by comparing to additional simulations performed using PBE [33] and vdW-DF [34] we also show that while the location of the phase boundary strongly depends on the functional, the isotope effect is not nearly as sensitive.

In this Letter we use the ring polymer path integral molecular dynamics (PIMD) technique [57] in combination with DFT to calculate the LLPT boundary for classical H_2 and quantum H_2/D_2 . We demonstrate the large isotopic shift by monitoring various properties of the system along five isotherms ranging from 1000 to 2500 K for both H_2 and D_2 . This isotope shift is impossible in classical physics, and is conclusive evidence of important NQEs at kiloKelvin temperatures.

One measure of the LLPT is the fraction of H_2 molecules present in the system. This can be obtained by tracking the height of the first peak in the radial distribution function (RDF), which corresponds to the molecular bond length. The results in Fig. 1(a) clearly show dissociation occurring for both H_2 and D_2 , as evidenced by a drop in peak height with increasing pressure. The relative sharpness and magnitude of this drop are temperature dependent, with the low temperature isotherms exhibiting the sharpest, largest drop and high temperature isotherms exhibiting smooth, small changes in peak height. The isotope effect is observed here as a shift in the phase boundary between H_2 and D_2 . This shift is on the order of 250 K.

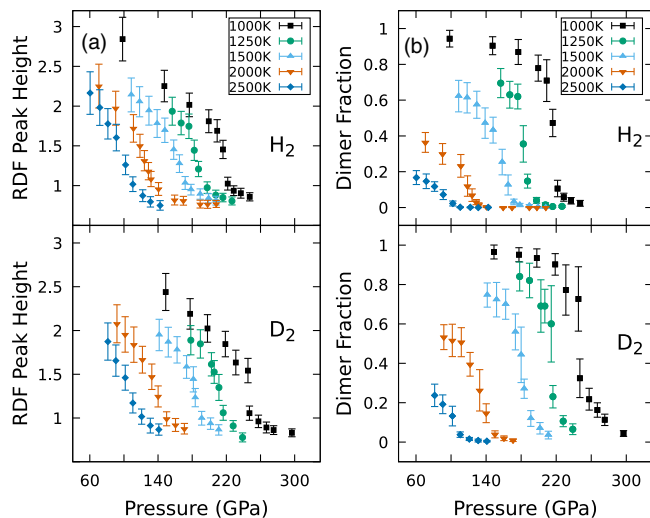


FIG. 1. Evidence of molecular dissociation. (a) Height of first (normalized) RDF peak, which corresponds to the molecular bond length. While the peak becomes relatively small, it does not disappear even in the atomic phase. (b) Fractions of H_2 and D_2 dimers present, where a stable dimer is defined as two H or D atoms that are less than 0.9 \AA apart for at least 85 fs. Example RDFs are shown in the Supplemental Material [26].

The change in RDF provides clear evidence of a transition, but does not explicitly consider the existence of molecules and does not distinguish between possible H_n clusters for n higher than 2. A more intuitive description of the dissociation can be found by considering the fraction of atoms that form a molecule. This is extracted from the interatomic distances, noting that the molecules continually break apart and reform, akin to a chemical reaction $H_2 \rightleftharpoons 2H$, which naturally introduces the idea of a molecular lifetime. We define a molecule to be two hydrogen or deuterium atoms less than 0.9 \AA apart for at least 85 fs. This allows for at least 10 vibrations in the case of hydrogen. This choice is motivated by the limits of experimental detectability: it corresponds to a spectroscopic natural linewidth of 400 cm^{-1} .

The resulting dimer fraction across the PIMD runs is shown in Fig. 1(b). The limiting cases of high and low temperatures show that the dimer fraction tends to the expected values of 0 and 1 in the atomic and molecular limits, although pressures near the transition here will have a sizable fraction of the liquid already dissociated. Like the RDF peak height, the dimer fraction drops steeply across the transition pressure for all isotherms. However, this drop can only be considered to be discontinuous around 1000 K for hydrogen and up to around 1250 K for deuterium; at higher temperatures the transitions become a crossover. This suggests that the critical point of the LLPT likely lies between 1000 and 1500 K for both isotopes, and is higher in deuterium.

The onset of dissociation is also marked by an increase in the diffusivity. Figure 2 shows calculated diffusion constants D for all isotherms, where it can be seen that D markedly increases in the high pressure atomic phase. The curves are qualitatively similar, allowing for the two times larger deuterium mass, but an isotope effect is seen in that the H_2 transition is shifted towards lower pressures. The results are qualitatively similar to results obtained previously in AIMD calculations [16,18] which showed that the

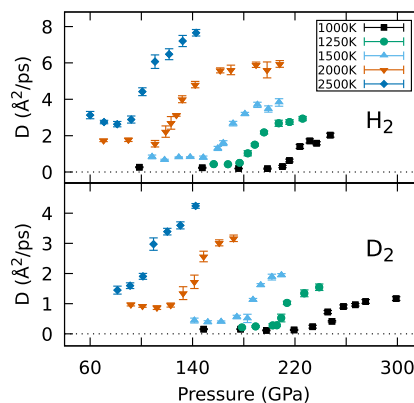


FIG. 2. Diffusion constant D as calculated from mean square displacements for H_2 and D_2 , showing evidence of increasing diffusivity across the dissociation with a clear isotope effect.

proton diffusivity increases rather than decreases with increasing pressure, meaning that the high pressure phase has lower viscosity. The diffusion constant remains nonzero in all simulations above the melt line and a close look at the mean squared displacement for these trajectories (shown in the Supplemental Material [26]) indicates that even at low temperatures, the simulations are indeed of a flowing liquid.

The LLPT is perhaps best thought of as a chemical reaction between distinct species H and H₂. This is in part because the transition is anomalous compared to first order transitions usually encountered, as there is no phase separation in the coexistence region: atomic and molecular hydrogen are continually interconverting, and therefore appear miscible [18]. Nevertheless, the location of the phase boundary can be established by considering various thermodynamic quantities. Since the system undergoes a small volume change across the isotherm either abruptly or gradually depending on the temperature, this will create a clear signature in the isothermal compressibility $\kappa_T = -(\partial V/\partial P)_T/V$. Here, it is estimated using the equilibrated NVT volumes and pressures using finite differences. These results are shown in Fig. 3(a), along with a fit to obtain the location of the peak. In theory, κ_T should diverge at a first-order transition and show a peak along an extension of the phase boundary beyond the critical point (the ‘‘Widom line’’). While this cannot happen in a finite sized system, the peaks can still be seen to be very sharp for both isotopes at low temperatures. For both

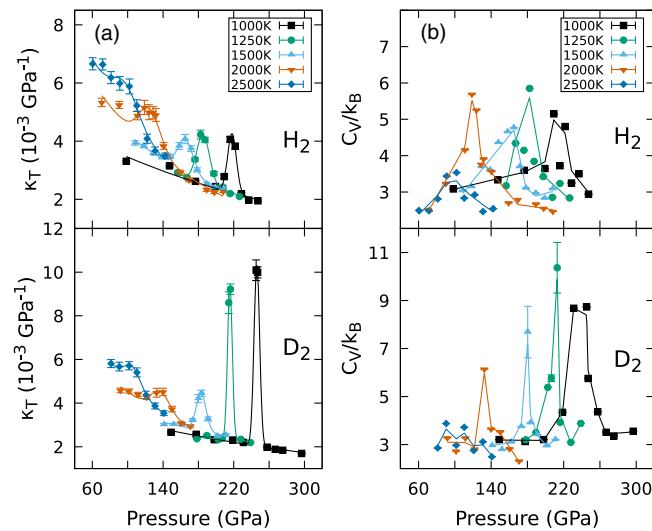


FIG. 3. (a) Estimated isothermal compressibility $\kappa_T = -(\Delta V/\Delta P)_T/V$ calculated using fixed volumes and equilibrated pressures for both isotopes. Solid lines are fits consisting of an exponential plus a Gaussian function. The center of the Gaussian peak was then used to establish the location of the phase boundary and Widom line. (b) Heat capacities of the full ring polymer systems for H₂ and D₂ established from fluctuations in energy estimators. Solid lines are a guide to the eye.

isotopes the peaks also widen at higher temperatures, which is indicative of a crossover rather than a phase transition.

The other thermodynamic quantity considered is the heat capacity at constant volume C_V , as this can be calculated directly from fluctuations in the internal energy. This should also diverge at a first-order transition and show a peak along the Widom line, due to the energy required to break the bonds. To calculate C_V in the PIMD formalism, some modifications must be made to account for interactions between beads. For these results, the centroid virial heat capacity is employed (see Supplemental Material [26]) to calculate the heat capacity of the full PIMD ring polymer system [35]. The results are shown in Fig. 3(b) for the various isotherms for both H₂ and D₂. The heat capacity is also clearly peaked like κ_T , but noisier due to it being a quantity obtained from fluctuations.

In both the quantities considered, the D₂ peaks are shifted compared to H₂ which further identifies the isotope effect. The magnitude of the peaks in both the heat capacity and compressibility is also larger in deuterium than hydrogen at lower temperatures. Both the quantities also show broadening of their respective peaks at higher temperatures, clearest in the compressibility, where the transition becomes a crossover rather than a thermodynamic phase transition.

The prevailing belief about the LLPT is that metallization and dissociation occur together [20,21], but, in principle, there is no reason that these two phenomena must coincide exactly. Furthermore, metallization can be observed at a distinctive pressure even beyond the critical point, perhaps by a percolation transition [58]. Onset of metallization in our simulations was monitored by calculating the Kubo-Greenwood conductivity [36] from snapshots taken from the PIMD trajectories. These results are shown in Fig. 4, where a minimum conductivity of 2000 S/cm was used to distinguish the metallic phase [7,59]. The conductivity steeply increases by 2 orders of

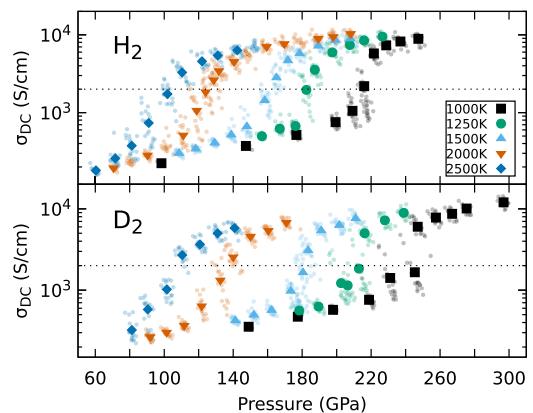


FIG. 4. Calculated dc electrical conductivity for H₂ and D₂ showing the onset of metallization. Scatter points are conductivities of individual samples. A tolerance of 2000 S/cm for metallization is indicated by dotted lines.

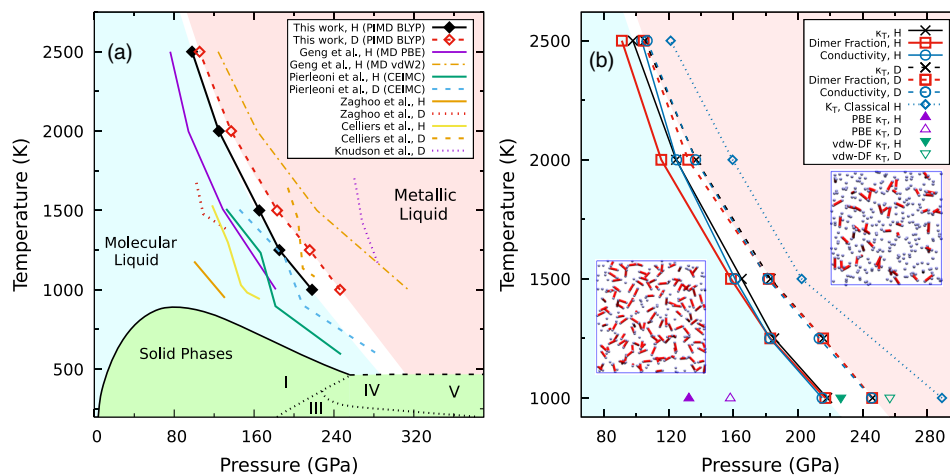


FIG. 5. Summary of the results obtained in this work. (a) Location of the phase boundary as established from peaks in the compressibility. The isotope effect is largest in magnitude at lower temperatures. Melting curve [61] and the likely continuation of the melting line beyond the I-IV-liquid triple point [62] shows where the LLPT phase line is expected to rejoin the solid phase lines. (b) Comparison of the compressibility phase line to the dissociation curve established from peaks in the gradient of the dimer fraction and the metallization line along with MD runs using classical H nuclei, all using BLYP. Additional NPT runs using PBE and vdW-DF functionals at 1000 K are also shown. Snapshots on either side of the transition are PIMD runs of H_2 at 1000 K using BLYP, for 100 and 250 GPa, with bonds highlighted in red.

magnitude at the transition pressure, coinciding very closely with dissociation in Fig. 1: hydrogen metallizes at lower temperature than deuterium. Our results show that at all temperatures hydrogen has higher conductivity than deuterium. Interestingly, this was noted experimentally by Weir *et al.* [7] but ascribed to a large difference in density, and the exact values remain uncertain [60].

The results are summarized in Fig. 5 on a PT phase diagram, established using peaks in the isothermal compressibility as this was found to give the most distinctive peaks. The Clapeyron slope is observed to be negative, which is consistent with the small but negative volume change across the transition. The volume change and Clapeyron slope are slightly larger for D_2 ; configurational entropy cannot be calculated precisely, but from volume and slope we estimate it to be about $k_B/2$ per molecule, consistent with the extra degree of freedom from breaking the bond. The isotope effect can be clearly observed as a shift in the transition pressure, which is largest in magnitude at lower temperatures where NQE effects are most significant.

The location of the phase boundary is largely influenced by two contributions. First, including NQE significantly lowers the transition pressure. This can be seen from complementary AIMD runs using BLYP and classical H nuclei shown in Fig. 5(b), where the phase boundary is obtained from the isothermal compressibility using identical methods to the PIMD runs.

Second, the location of the LLPT is very sensitive to the choice of exchange-correlation functional, which can shift the whole phase boundary by as much as 100 GPa [18]. This is mainly due to the well-known tendency of the

PBE-based functionals [33] towards easy metallization compared with functionals which correctly describe the high density-gradient limit [29]. Additional PIMD runs, shown in Fig. 5(b) (further discussed in the Supplemental Material [26]), reveal a similarly significant spread in the location of the phase boundary.

Nevertheless, the isotope shift is found to be far less sensitive to the choice of functional (in contrast to other systems with significant NQE such as liquid water [21]), giving a shift of almost 30 GPa at 1000 K. The magnitude of the isotope effect is smaller than observed in experiments by Zaghou *et al.* [5], but more similar to CEIMC simulations.

The critical point is difficult to locate with MD. The discontinuous changes in thermodynamic properties below the critical point are blurred by finite size effects, and anomalous peaks remain along the Widom lines beyond T_c . Both the molecular dissociation and metallization curves match up with the thermodynamic phase boundary below the critical point, and thus also exhibit a quantitatively similar isotope effect, but beyond this the dissociation line in particular occurs at slightly lower pressures than the Widom line.

We have shown the existence of a strong isotope effect of several hundred Kelvins in the liquid-liquid transition in hydrogen, with the transformation occurring at lower temperatures and pressures in hydrogen than deuterium, and much lower than in previous work using classical nuclei. There is no such effect at the melt line, nor (by definition) in Born-Oppenheimer dynamics. So we can confidently ascribe it to the different zero-point energy of hydrogen and deuterium vibrations; the difference in these

$\frac{1}{2}\hbar(\omega_H - \omega_D)$ has the appropriate order of magnitude of hundreds of Kelvin.

The strong dependence of the calculated LLPT line on the exchange-correlation functional makes it impossible to confidently state the precise location of the LLPT. Moreover, above the critical point the transition becomes a crossover and the associated Widom lines depend on the precise quantity being measured. In this work, the magnitude of the isotope effect is likely to be more accurate than the exact location of the LLPT line. While the exact location of the boundary will likely remain contentious until experimental results can pin it down more accurately, *ab initio* PIMD methods are clearly effective in showing that an isotope effect is indeed present in the LLPT. They also emphasize that experiments on deuterium cannot be used as a proxy for the hydrogen phase diagram.

It is well known that the quantum effects are only important at “low” temperatures. We show here that low temperature must be interpreted in terms of the relevant quantum energy scales, which for molecular vibration modes can mean shifts in phase boundaries of hundreds of Kelvins at temperatures of thousands of Kelvins. These conclusions have general applicability to other molecular-dissociation transitions, such as nitrogen and superionic ammonia and water [9,63–65], meaning that experiments on deuterated samples will significantly overestimate the transition pressures and temperatures compared with the natural material.

Data for this work publicly available under the Ref. [66].

We acknowledge the support of the ERC grant HECATE and studentship funding from EPSRC under grant ref EP/L015110/1. This work used the Cirrus UK National Tier-2 HPC Service at EPCC funded by the University of Edinburgh and EPSRC (EP/P020267/1). We are grateful for computational support from the UK national high performance computing service, ARCHER, for which access was obtained via the United Kingdom Car-Parrinello (UKCP) consortium and funded by EPSRC grant ref EP/P022561/1.

[1] R. P. Dias and I. F. Silvera, *Science* **355**, 715 (2017).
 [2] P. Loubeyre, F. Occelli, and P. Dumas, *Nature (London)* **577**, 631 (2020).
 [3] V. Dzyabura, M. Zaghoo, and I. F. Silvera, *Proc. Natl. Acad. Sci. U.S.A.* **110**, 8040 (2013).
 [4] M. Zaghoo, A. Salamat, and I. F. Silvera, *Phys. Rev. B* **93**, 155128 (2016).
 [5] M. Zaghoo, R. J. Husband, and I. F. Silvera, *Phys. Rev. B* **98**, 104102 (2018).
 [6] S. Jiang, N. Holtgrewe, Z. M. Geballe, S. S. Lobanov, M. F. Mahmood, R. S. McWilliams, and A. F. Goncharov, *Adv. Sci.* **7**, 1901668 (2020).
 [7] S. T. Weir, A. C. Mitchell, and W. J. Nellis, *Phys. Rev. Lett.* **76**, 1860 (1996).

[8] M. Knudson, M. Desjarlais, A. Becker, R. Lemke, K. Cochran, M. Savage, D. Bliss, T. Mattsson, and R. Redmer, *Science* **348**, 1455 (2015).
 [9] P. M. Celliers, M. Millot, S. Brygoo, R. S. McWilliams, D. E. Fratanduono, J. R. Rygg, A. F. Goncharov, P. Loubeyre, J. H. Eggert, J. L. Peterson, N. B. Meezan, S. Le Pape, G. W. Collins, R. Jeanloz, and R. J. Hemley, *Science* **361**, 677 (2018).
 [10] A. Becker, N. Nettelmann, U. Kramm, W. Lorenzen, M. French, and R. Redmer, *Proc. Int. Astron. Union* **6**, 473 (2010).
 [11] D. C. Swift, J. Eggert, D. G. Hicks, S. Hamel, K. Caspersen, E. Schwegler, G. W. Collins, N. Nettelmann, and G. Ackland, *Astrophys. J.* **744**, 59 (2012).
 [12] G. Chabrier, S. Mazevet, and F. Soubiran, *Astrophys. J.* **872**, 51 (2019).
 [13] J. M. McMahon, M. A. Morales, C. Pierleoni, and D. M. Ceperley, *Rev. Mod. Phys.* **84**, 1607 (2012).
 [14] S. Scandolo, *Proc. Natl. Acad. Sci. U.S.A.* **100**, 3051 (2003).
 [15] B. Holst, R. Redmer, and M. P. Desjarlais, *Phys. Rev. B* **77**, 184201 (2008).
 [16] W. Lorenzen, B. Holst, and R. Redmer, *Phys. Rev. B* **82**, 195107 (2010).
 [17] M. A. Morales, J. M. McMahon, C. Pierleoni, and D. M. Ceperley, *Phys. Rev. Lett.* **110**, 065702 (2013).
 [18] H. Y. Geng, Q. Wu, M. Marqués, and G. J. Ackland, *Phys. Rev. B* **100**, 134109 (2019).
 [19] M. A. Morales, C. Pierleoni, E. Schwegler, and D. Ceperley, *Proc. Natl. Acad. Sci. U.S.A.* **107**, 12799 (2010).
 [20] G. Mazzola and S. Sorella, *Phys. Rev. Lett.* **114**, 105701 (2015).
 [21] C. Pierleoni, M. A. Morales, G. Rillo, M. Holzmann, and D. M. Ceperley, *Proc. Natl. Acad. Sci. U.S.A.* **113**, 4953 (2016).
 [22] G. Rillo, M. A. Morales, D. M. Ceperley, and C. Pierleoni, *Proc. Natl. Acad. Sci. U.S.A.* **116**, 9770 (2019).
 [23] B. Cheng, G. Mazzola, C. J. Pickard, and M. Ceriotti, *Nature (London)* **585**, 217 (2020).
 [24] X.-D. Liu, P. Dalladay-Simpson, R. T. Howie, H.-C. Zhang, W. Xu, J. Binns, G. J. Ackland, H.-K. Mao, and E. Gregoryanz, *Proc. Natl. Acad. Sci. U.S.A.* **117**, 13374 (2020).
 [25] K. K. Irikura, *J. Phys. Chem. Ref. Data* **36**, 389 (2007).
 [26] See Supplemental Material at <http://link.aps.org/supplemental/10.1103/PhysRevLett.126.225701> for discussion of previous studies of the LLPT, a tabular comparison of major existing *ab initio* studies and their simulation parameters, details on the computational methods employed, PIMD bead convergence, sample radial distribution functions, sample mean square displacements, band gaps, PV equations of state, and additional simulations using other exchange-correlation functionals, including Refs. [5,6,8,16–18,21,23,27–55].
 [27] M. A. Morales, C. Pierleoni, and D. M. Ceperley, *Phys. Rev. E* **81**, 021202 (2010).
 [28] G. J. Ackland and I. B. Magdǎu, *Cogent Phys.* **2**, 1049477 (2015).
 [29] S. Azadi and G. J. Ackland, *Phys. Chem. Chem. Phys.* **19**, 21829 (2017).
 [30] A. D. Becke, *Phys. Rev. A* **38**, 3098 (1988).
 [31] C. Lee, W. Yang, and R. G. Parr, *Phys. Rev. B* **37**, 785 (1988).

- [32] R. C. Clay III, J. Mcminis, J. M. McMahon, C. Pierleoni, D. M. Ceperley, and M. A. Morales, *Phys. Rev. B* **89**, 184106 (2014).
- [33] J. P. Perdew, K. Burke, and M. Ernzerhof, *Phys. Rev. Lett.* **77**, 3865 (1996).
- [34] M. Dion, H. Rydberg, E. Schröder, D. C. Langreth, and B. I. Lundqvist, *Phys. Rev. Lett.* **92**, 246401 (2004).
- [35] K. R. Glaesemann and L. E. Fried, *J. Chem. Phys.* **117**, 3020 (2002).
- [36] L. Calderin, V. V. Karasiev, and S. B. Trickey, *Comput. Phys. Commun.* **221**, 118 (2017).
- [37] S. Biermann, D. Hohl, and D. Marx, *J. Low Temp. Phys.* **110**, 97 (1998).
- [38] S. Biermann, D. Hohl, and D. Marx, *Solid State Commun.* **108**, 337 (1998).
- [39] H. Y. Geng, H. X. Song, J. Li, and Q. Wu, *J. Appl. Phys.* **111**, 063510 (2012).
- [40] H. Y. Geng, R. Hoffmann, and Q. Wu, *Phys. Rev. B* **92**, 104103 (2015).
- [41] I. B. Magdău and G. J. Ackland, [arXiv:1511.05173](https://arxiv.org/abs/1511.05173).
- [42] I. B. Magdău and G. J. Ackland, in *Journal of Physics: Conference Series*, Vol. 950 (IOP Publishing, London, 2017), p. 042058, <https://iopscience.iop.org/article/10.1088/1742-6596/950/4/042058>.
- [43] B. Lu, D. Kang, D. Wang, T. Gao, and J. Dai, *Chin. Phys. Lett.* **36**, 103102 (2019).
- [44] J. Hinz, V. V. Karasiev, S. X. Hu, M. Zaghoo, D. Mejía-Rodríguez, S. B. Trickey, and L. Calderin, *Phys. Rev. Research* **2**, 032065(R) (2020).
- [45] C. Tian, F. Liu, H. Yuan, H. Chen, and Y. Gan, *J. Phys. Condens. Matter* **33**, 015401 (2021).
- [46] V. Kapil *et al.*, *Comput. Phys. Commun.* **236**, 214 (2019).
- [47] P. Giannozzi *et al.*, *J. Phys. Condens. Matter* **29**, 465901 (2017).
- [48] A. Baldereschi, *Phys. Rev. B* **7**, 5212 (1973).
- [49] S. Azadi and W. M. C. Foulkes, *Phys. Rev. B* **88**, 014115 (2013).
- [50] M. Ceriotti, M. Parrinello, T. E. Markland, and D. E. Manolopoulos, *J. Chem. Phys.* **133**, 124104 (2010).
- [51] M. Ceriotti, J. More, and D. E. Manolopoulos, *Comput. Phys. Commun.* **185**, 1019 (2014).
- [52] D. J. Chadi and M. L. Cohen, *Phys. Rev. B* **8**, 5747 (1973).
- [53] D. R. Hamann, M. Schlüter, and C. Chiang, *Phys. Rev. Lett.* **43**, 1494 (1979).
- [54] K. Laasonen, A. Pasquarello, R. Car, C. Lee, and D. Vanderbilt, *Phys. Rev. B* **47**, 10142 (1993).
- [55] Wang, M. Ceriotti, and T. E. Markland, *J. Chem. Phys.* **141**, 104502 (2014).
- [56] I. B. Magdău, F. Balm, and G. J. Ackland, *J. Phys. Conf. Ser.* **950**, 042059 (2017).
- [57] D. Marx and J. Hutter, *Ab Initio Molecular Dynamics: Basic Theory and Advanced Methods* (Cambridge University Press, New York, 2009).
- [58] I. B. Magdău, M. Marques, B. Borgulya, and G. J. Ackland, *Phys. Rev. B* **95**, 094107 (2017).
- [59] W. J. Nellis, S. T. Weir, and A. C. Mitchell, *Phys. Rev. B* **59**, 3434 (1999).
- [60] M. Zaghoo and I. F. Silvera, *Proc. Natl. Acad. Sci. U.S.A.* **114**, 11873 (2017).
- [61] R. T. Howie, P. Dalladay-Simpson, and E. Gregoryanz, *Nat. Mater.* **14**, 495 (2015).
- [62] P. Dalladay-Simpson, R. T. Howie, and E. Gregoryanz, *Nature (London)* **529**, 63 (2016).
- [63] M. Millot, F. Coppari, J. R. Rygg, A. C. Barrios, S. Hamel, D. C. Swift, and J. H. Eggert, *Nature (London)* **569**, 251 (2019).
- [64] S. Jiang, N. Holtgrewe, S. S. Lobanov, F. Su, M. F. Mahmood, R. S. McWilliams, and A. F. Goncharov, *Nat. Commun.* **9**, 1 (2018).
- [65] V. N. Robinson and A. Hermann, *J. Phys. Condens. Matter* **32**, 184004 (2020).
- [66] <https://doi.org/10.7488/ds/3042>.